Reprinted from Inorganic Chemistry, 1994, *33*.

Effect of Diverse Ligands on the Course of a Molecules-to-Solids Process and Properties of Its Intermediates

M. L. Steigerwald,* T. Siegrist, E. M. Gyorgy, B. Hessen,[†] Y.-U. Kwon,[‡] and S. M. Tanzler

AT&T Bell Laboratories, 600 Mountain Avenue, Murray Hill, New Jersey 07974

Received February 23, 1994[⊗]

We have been studying chemical processes that use discrete molecular reagents to form extended solid inorganic materials. The goals of this program have been to determine how best to design and implement these molecular precursor reactions and to discover what chemical intermediates lie on the molecules-to-solids paths. In this manuscript we report studies of the reactions of the low-valent iron complex $Fe(C_8H_8)_2$ with low-valent tellurium compounds of the form $TePR_3$ (R = various hydrocarbon groups) that lead ultimately to the exclusively inorganic extended solid compounds Fe_xTe_y. We have found four Fe/Te cluster types that are chemical intermediates in this process: $Fe_4Te_4(PEt_3)_4$, **1**; $Fe_4Te_4(P^iPr_3)_4$, **2**; $Fe_6Te_8(PMe_3)_6$, **3**; $(dmpe)_2FeTe_2$, **4**; $(depe)_2FeTe_2$, **5**; $Fe_4Te_6(dmpe)_4$, **6**. (Here ^{i}Pr = $CHMe_2$, dmpe = $Me_2PCH_2CH_2PMe_2$, and depe = $Et_2PCH_2CH_2PEt_2$.) The different clusters form when different supporting phosphine ligands are employed. We report the syntheses, structures, and properties of these intermediates and the comparisons and contrasts between these molecular intermediates and the extended solid products. We note that when larger ligands are used smaller clusters are formed. We also note what features of the molecular structures lead to ferromagnetic versus antiferromagnetic coupling of the distinct Fe centers. We have determined the structures of the following materials crystallographically: **2** ($C_{36}H_{84}Fe_4Te_4P_4$; tetragonal, *P*42̄1c; *a* = 14.0469(7) Å, *c* = 13.5418(9) Å; *Z* = 2); **3** ($C_{18}H_{54}Fe_6Te_8P_6$; trigonal, *R*3; *a* = 11.859(2) Å, *c* = 26.994(5) Å; *Z* = 3); dmpe·2Te ($C_6H_{16}Te_2P_2$; monoclinic, $P2_1/c$; *a* = 6.0890(4) Å, *b* = 10.7934(7) Å, *c* = 9.8200(5) Å, *b* = 104.63(7)°; *Z* = 2); **5** ($C_{20}H_{48}FeTe_2P_4$; orthorhombic, *Pbnn*; *a* = 10.997(3) Å, *b* = 14.157(3) Å, *c* = 18.345(4) Å; *Z* = 4); **6** ($C_{24}H_{64}Fe_4Te_6P_8$; orthorhombic, *Abaa*; *a* = 12.056(3) Å, *b* = 17.725(5) Å, *c* = 21.403(8) Å; *Z* = 4).

Introduction

The study of chemical processes that lead from molecular reagents to extended solid products has several goals. Among these is the determination of methods by which the otherwise runaway reactions can be controlled in a purposeful way. Were the appropriate methods of control available, one could envision the construction of very complex solids *via* strictly chemical means. At present such a level of fine control is not generally available.

In the present manuscript we describe our efforts to control the processes that lead from the initial combination of bis(cyclooctatetraene)iron, $Fe(COT)_2$, and triethylphosphine telluride, $TePEt_3$, to the ultimate products, solid-state tellurides of iron, Fe_xTe_y. We find that the addition of different phosphine ligands to the reaction mixture results in the formation of different Fe/Te-containing molecular compounds. We describe the syntheses of these materials, their molecular structures and properties, and their physical and chemical relationships among one another and to the associated extended solids.

Experimental Section

Unless noted to the contrary all manipulations were conducted under inert atmosphere using conventional techniques. Triethylphosphine (PEt_3, Aldrich), trimethylphosphine (PMe_3, 1 M solution in toluene, Aldrich), triisopropylphosphine (P^iPr_3 Strem), bis(dimethylphosphino)ethane (dmpe, Strem), bis(diethylphosphino)ethane (depe, Strem), and tellurium (Aldrich) were used as received. Solvents were anhydrous and used as received from Aldrich. Simple trialkylphosphine tellurides[1] and bis(cyclooctatetraene)iron[2] were prepared using literature methods. Magnetic susceptibility measurements were made on a SQUID magnetometer using standard techniques.

Synthesis of $Fe_4Te_4(P^iPr_3)_4$, 2. $Fe(COT)_2$ (1.00 g, 3.79 mmol) dissolved in toluene (15 mL) was treated with a mixture of TeP^iPr_3 (1.09 g, 3.79 mmol) and P^iPr_3 (1.82 g, 11.4 mmol) in toluene (15 mL). The resulting solution was heated to reflux 4.5 h, after which the deep brown mixture was cooled to room temperature and filtered through a medium-porosity glass frit. The solution was condensed *in vacuo* to roughly half its original volume. Cooling this latter solution to -20 °C overnight gave crystallization of $Fe_4Te_4(P^iPr_3)_4$ that was isolated, washed with pentane (2 × 5 mL), and dried (0.293 g, 8.53×10^{-5} mol, 23%). Anal. Calcd for $C_{36}H_{84}Fe_4P_4Te_4$: C, 31.45; H, 6.16; Fe, 16.25; P, 9.01; Te, 37.13. Found: C, 31.57; H, 6.12; Fe, 16.50; P, 8.83; Te, 37.05.

Synthesis of $Fe_6Te_8(PMe_3)_6$, 3. A solution of $Fe(COT)_2$ (1.00 g, 3.79 mmol) in toluene was distributed equally in three vials. Additional toluene (3 × 10mL) was carefully layered onto each. In a separate vessel elemental Te (0.65 g, 5.1 mmol) was dissolved in a solution of PMe_3 in toluene/pentane (13 g of a stock 1 M toluene solution of PMe_3 plus an additional 10 mL of toluene and 15 mL of pentane). The phosphine telluride solution was filtered and then layered evenly onto each of the three $Fe(COT)_2$ solutions. After 3 days at room temperature the layers had interdiffused and crystals of $Fe_6Te_8(PMe_3)_6$ had formed. This solid was isolated, washed (2 × 5 mL of pentane), and dried (0.12 g, 6.6×10^{-5} mol, 10%). Anal. Calcd for $C_{18}H_{54}Fe_6P_6Te_8$: C, 11.93; H, 3.00; Fe, 18.49; P, 10.25; Te, 56.32. Found: C, 12.20; H, 2.91; Fe, 18.55; P, 10.15; Te, 56.40.

Pyrolysis of $Fe_6Te_8(PMe_3)_6$. A Pyrex ampule was charged with $Fe_6Te_8(PMe_3)_6$ (0.044 g, 0.024 mmol), connected through a liquid-nitrogen trap to a vacuum pump, and heated to 170 °C for 5 min. During this time the trimethylphosphine evolved as evidenced by the increase and subsequent decrease in the observed pressure. The residual solid (0.033 g, corresponding to 100% PMe_3 loss) was sealed in an evacuated Pyrex tube and annealed for 2 h at 350 °C. The residual solid was collected, washed with pentane, and dried *in vacuo* (0.030 g). Powder X-ray diffraction showed this to be a mixture of *b*- and *e*-FeTe.[3,4] (N.B., during the annealing process a small amount of Te was transported to the cool end of the tube. This accounts for the small mass loss.)

Synthesis of dmpe·2Te. A solution of dmpe (0.15 g, 1.0 mmol) in toluene (5 mL) was treated with a solution of $TePEt_3$ (0.5 g, 2 mmol)

[†] Present address: Koninklijke Shell Laboratorium Amsterdam, P. O. Box 3003, NL-1003, AA Amsterdam, The Netherlands.

[‡] Present address: Department of Chemistry, Sung Kyun Kwan University, Suwon, Korea.

[⊗] Abstract published in *Advance ACS Abstracts*, June 15, 1994.

(1) Zingaro, R. A.; Stevens, B. H.; Irgolic, K. *J. Organomet. Chem.* **1965**, *4*, 320.

(2) Gerlach, D. H.; Schunn, R. A. *Inorg. Synth.* **1971**, *15*, 2.

(3) Grønvold, F.; Haraldsen, H.; Vihovde, J. *Acta Chem. Scand.* **1954**, *8*, 1927. The phase designations used in the present manuscript are those suggested in this reference.

(4) Ipser, H.; Komarck, K. L.; Mikler, H. *Monatsh. Chem.* **1974**, *105*, 1322.

0020-1669/94/1333-3389$04.50/0

Table 1. Crystallographic Data for $Fe_4Te_4(P^iPr_3)_4$, $Fe_6Te_8(PMe_3)_6$, dmpe·2Te, $FeTe_2(depe)_2$, and $Fe_4Te_6(dmpe)_4$

	$Fe_4Te_4(P^iPr_3)_4$	$Fe_6Te_8(PMe_3)_6$	mpe·2Te	$FeTe_2(depe)_2$	$Fe_4Te_6(dmpe)_4$
chem formula	$Fe_4Te_4P_4C_{36}H_{84}$	$Fe_6Te_8P_6C_{18}H_{54}$	$Te_2P_4C_6H_{16}$	$FeTe_2P_4C_{20}$	$Fe_4Te_6P_8C_{24}H_{64}$
fw	1374.75	1812.35	405.35	675.16	1589.56
space group	*P*421*c*	*R*3	$P2_1/c$	*Pbnm*	*Abaa*
a (Å)	14.0469(7)	11.859(2)	6.0890(4)	10.997(3)	12.056(3)
b (Å)			10.7934(7)	14.157(3)	17.725(5)
c (Å)	13.5418(9)	26.994(5)	9.8200(5)	18.345(4)	21.403(8)
b (deg)			104.63(7)		
V (Å^3)	2672.0(3)	3287.7(8)	621.63(7)	2856(1)	4574(3)
Z	2	3	2	4	4
T (°C)	23	23	23	23	23
r_{calc} (g/cm^3)	1.71	2.75	2.17	1.57	2.31
m (mm^{-1})	3.35	8.12	4.91	2.76	4.04
λ (Å)	0.709 30	0.709 30	0.709 30	0.709 30	0.709 30
R_f[a]	0.053	0.022	0.027	0.041	0.033
R_w[b]	0.059	0.021	0.029	0.046	0.043

[a] $R_f = \Sigma(F_o - F_c)/\Sigma F_o$. [b] $R_w = \Sigma w(F_o - F_c)^2/\Sigma(wF_o^2)$.

in toluene (5 mL). The precipitation of dmpe·2Te began immediately. The mixture was left undisturbed several hours. The pale yellow microcrystalline solid was isolated by filtration, washed with pentane (3 × 5 mL), and dried (0.23 g, 0.51 mmol, 51%). Anal. Calcd for $C_6H_{16}P_2Te_2$: C, 17.78; H, 3.98; P, 15.28; Te, 62.96. Found: C, 17.80; H, 3.94; P, 15.52; Te, 62.70. This compound is quite insoluble in toluene and pentane but is soluble in toluene to which several equivalents of PEt_3 have been added. Crystals suitable for diffraction were prepared by allowing the same two solutions to interdiffuse slowly at room temperature.

Synthesis of $(dmpe)_2FeTe_2$, 4. A solution of $Fe(COT)_2$ (0.264 g, 1.0 mmol) in toluene (10 mL) was treated with a solution of dmpe (0.30 g, 2.0 mmol), $TePEt_3$ (0.49 g, 2.0 mmol), and PEt_3 (0.80 g, 6.8 mmol) in toluene (20 mL). The resulting mixture was filtered into a Schlenk tube and subsequently evaporated to dryness *in vacuo*. The resulting solid was extracted with toluene (15 mL). The extract was condensed and cooled to-20 °C, at which point crystallization of $(dmpe)_2FeTe_2$ occurred. The solid was isolated, washed (2 × 5 mL of pentane), and dried (0.14 g, 0.23 mmol, 23%). Anal. Calcd for $C_{12}H_{32}FeP_4Te_2$: C, 23.58; H, 5.28; Fe, 9.14; P, 20.27; Te, 41.75. Found: C, 23.86; H, 5.28; Fe, 9.30; P, 20.03; Te, 41.65. UV-visible absorption (toluene): λ_{max} = 478, 584, 782 nm.

Pyrolysis of $(dmpe)_2FeTe_2$. A Schlenk tube was charged with $(dmpe)_2FeTe_2$ (44 mg, 7.2×10^{-5} mol). While the tube was open to vacuum (approximately 0.1 Torr), it was plunged into an oil bath whose temperature had been adjusted to 210 °C. As indicated by the vacuum gauge, volatile material evolved as the solid changed appearance from dark red to metallic black. After 25 min, the tube was cooled and the solid collected (23 mg; complete removal of dmpe from 44 mg of $(dmpe)_2FeTe_2$ would leave 22 mg of solid). X-ray powder diffraction by showed only $FeTe_2$.[3,4]

Synthesis of $(depe)_2FeTe_2$. 5. A solution of $Fe(COT)_2$ (264 mg, 1.0 mmol) in toluene (13 mL) was treated with a solution of depe (412 mg, 2.0 mmol) and $TePEt_3$ (491 mg, 2.0 mmol) in toluene (10 mL). The resulting solution was agitated to ensure complete mixing and then was left at room temperature overnight. At this point the volatile components of the mixture were removed *in vacuo* and the resulting dark, sticky solid was washed with pentane (15 mL), dried, and subsequently extracted with toluene (10 mL). The extract was condensed to approximately half is original volume and then cooled to-20 °C. The densely colored product formed as a crystalline solid (0.22 g, 30%). Anal. Calcd for $C_{20}H_{48}FeP_4Te_2$: C, 33.20; H, 6.69; Fe, 7.72; P, 17.12; Te, 35.27. Found: C, 33.08; H, 6.63; Fe, 7.86; P, 16.94; Te, 35.50. This compound is soluble in toluene and thf. UV-vis absorption (toluene): λ_{max} = 498, 615, 772 nm.

Synthesis of $Fe_4Te_6(dmpe)_4$, 6. A solution of $Fe(COT)_2$ (0.27 g, 1.0 mmol) in toluene (5 mL) was treated with a solution of dmpe (0.15 g, 1.0 mmol) in toluene (5 mL), and the combined solution was filtered. A solution of $TePEt_3$ (0.25 g, l.0 mmol) in toluene (5 mL) was carefully layered onto the Fe-containing solution. The resulting mixture was left undisturbed at room temperature for 5 days, during which time crystals of $(dmpe)_4Fe_4Te_6$ formed. The supernatant solution was decanted, and the solid was washed thoroughly (5 × 1 mL of toluene, 5 × 1 mL of pentane). Drying gave 10.0 mg (6.3×10^{-6} mol, 2.5%). This solid is absolutely insoluble in toluene, thf, and pentane. The crystals formed by this procedure can be used directly for X-ray crystallography.

X-ray Crystallography. In each of the systems for which we determined structures crystallographically a suitable crystal was mounted in a Lindemann capillary in an inert-atmosphere drybox. Diffraction data were collected on an Enraf-Nonius CAD4 diffractometer using graphite-monochromatized Mo K*a* radiation and the NRCCAD program package.[5] The diffraction data are summarized in Table 1. Calculations were performed using the NRCVAX program package.[6] Absorption corrections were applied in each case. In each case the structure was solved by direct methods.

Disorder of the isopropyl carbon atoms was found in $Fe_4Te_4(P^iPr_3)_4$. Although an ordered model could be refined, the difference Fourier maps clearly indicated rotational disorder of the P^iPr_3 groups.

Results

We have previously reported[7] that the reaction of $Fe(COT)_2$ with $TePEt_3$ in the presence of additional PEt_3 yields the cluster compound $Fe_4Te_4(PEt_3)_4$, **1**. The structure of this compound is a tetrahedron of four Fe atoms in which each tetrahedral face is capped with a triply-bridging Te atom. The structure is completed by four phosphine ligands, one coordinated to each Fe. We sought the answer to the question of how strongly the nature of the cluster product resulting from the combination of $Fe(COT)_2$ with phosphine tellurides depends on the supporting ligand by conducting a series of similar reactions in which we simply varied the phosphine.

When we used P^iPr_3 in place of PEt_3, the first observation was that the Fe/Te reaction required more forcing conditions. While $Fe(COT)_2$ and $TePEt_3$ react upon combination at room temperature, the same iron compound reacts with TeP^iPr_3 only on heating to reflux in toluene. After this reaction mixture had been at reflux for 4.5 h, it was cooled, filtered, and condensed. The cluster product $Fe_4Te_4(P^iPr_3)_4$, **2**, formed as a crystalline solid (eq 1). We determined the structure of this compound by

$$Fe(COT)_2 + TeP^iPr_3 \rightarrow Fe_4Te_4(P^iPr_3)_4 \qquad (1)$$

X-ray crystallography (Tables 1 and 2, and Figure 1) and found that it is essentially that of **1**, i.e., formed by concentric Fe_4Te_4 and P_4 tetrahedra. Compound **2** is thus the latest member of the large family of Fe_4E_4 cubane cluster compounds[8-15] and of the

(5) LePage, Y.; White, P. S.; Gabe, E. J. *Proc. Am. Cryst. Assoc. Annu. Meeting 1986*; Hamilton, Canada; AIP: New York, 1986; Poster PA23.
(6) Gabe, E. J.; Lee, F. L.; LePage, Y.; Charland, J. P.; Lee, F. L.; White, P. S. *J. Appl. Crystallogr.* **1989**, *22*, 384.
(7) Steigerwald, M. L.; Siegrist, T. S.; Stuczynski, S. M.; Kwon, Y.-U. *J. Am. Chem. Soc.* **1992**, *114*, 3155. See also: Cecconi, F.; Ghilardi, C. A.; Midollini, S.; Orlandini, A. *J. Chem. Soc., Chem. Commun.* **1992**, 910.
(8) Holm, R. H.; Ciurli, S.; Weigel, J. A. *Prog. Inorg. Chem.* **1990**, *38*, 1.
(9) Weigel, J. A.; Holm, R. H. *J. Am. Chem. Soc.* **1991**, *113*, 4184 and references therein.
(10) Zanello, P. *Coord. Chem. Rev.* **1988**, *83*, 199.
(11) Schunn, R. A.; Fritchie, C. J., Jr.; Prewitt, C. T. *Inorg. Chem.* **1966**, *5*, 892.
(12) Wei, C. H.; Wilkes, G. R.; Treichel, P. M.; Dahl, L. F. *Inorg. Chem.* **1966**, *5*, 900.

Table 2. Structural Comparison of $Fe_4Te_4(P^iPr_3)_4$ and $Fe_4Te_4(PEt_3)_4$[a]

Distances (Å)

ligand	Fe-Fe	Fe-Te	Fe-P
P^iPr_3	2.687(5)	2.623(3)	2.447(6)
	2.675(5)	2.620(3)	
	2.687(5)	2.614(3)	
PEt_3	2.623(4)	2.609(1)	2.390(6)

Angles (deg)

ligand	Fe-Te-Fe	Te-Fe-Te
P^iPr_3	61.73(7)	112.71(9)
	61.36(7)	111.62(9)
	61.77(8)	111.71(9)
PEt_3	60.36(6)	112.70(5)

[a] Data concerning $Fe_4Te_4(PEt_3)_4$ were taken from ref 6.

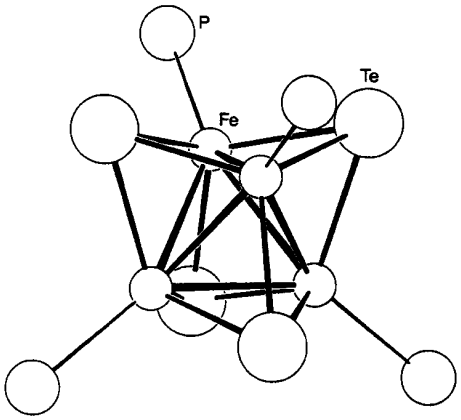

Figure 1. Structure of $Fe_4Te_4(P^iPr_3)_4$, **2**. The largest circles represent Te atoms, the smallest circles represent Fe atoms, and the medium circles represent the P atoms of the P^iPr_3 ligands. Selected distances and angles are given in Table 2.

much smaller family of Fe_4Te_4 compounds.[16-19] The data in Table 2 show that the bond distances in **2** are generally longer than the corresponding distances in **1**. This is best explained by the greater steric bulk of P^iPr_3. While **1** is crystallographically cubic, **2** is distorted from this ideal. This is ultimately due to the structural asymmetry of P^iPr_3. The cluster **2** differs from **1** in solubility; while **1** is only slightly soluble in toluene, **2** is exceedingly so. Both the sluggish reactivity of TeP^iPr_3 and the increased solubility of **2** can be rationalized by the bulk of the triisopropylphosphine ligands.

Since an increase in the size of the phosphine gave the same cluster core, the effect of a comparable decrease in phosphine size was at issue. When $Fe(COT)_2$ is treated with a mixture of $TePMe_3$ and PMe_3, and the solutions of the Fe and Te reagents are allowed to interdiffuse slowly, a cluster product, **3**, appears as large crystals. We determined the structure of **3** and found that it has a Fe_6Te_8 core and not the Fe_4Te_4 core of **1** and **2**. The crystallographic data collection is reviewed in Table 1, and the structure of the cluster is summarized in Table 3 and Figure 2.

Table 3. Selected Interatomic Distances (Å) and Angles (deg) in $Fe_6Te_8(PMe_3)_6$[a]

Distances

Fe-Te1a	2.541(1)	Te1a-Te1c′	3.684(1)
Fe-Te1b	2.544(1)	Te1-Te2	3.485(1)
Fe-Te1c	2.542(2)		
Fe-Te2	2.566(1)	$(Fe\text{-}Te)_{vic}$[b]	2.548
Fe-Fe*	2.818(2)	$(Fe\text{-}Fe)_{vic}$[b]	2.895
Fe-Fe#	2.972(2)	$(Te\text{-}Te)_{vic}$[b]	3.585
Fe-P	2.245(2)		

Angles around Fe

Te1a-Fe-Te2	86.06(2)	Te1b-Fe-Te2	86.02(2)
Te1b-Fe-Te1c′	92.83(3)	Te1b-Fe-P	90.79(5)
Te1a-Fe-P	94.32(5)	Te1a-Fe-Te1c′	92.83(3)
Te2-Fe-P	102.94(5)	Te1c′-Fe-Te2	166.27(3)
Te1a-Fe-Te1b	168.42(4)	Te1c′-Fe-P	95.67(5)

Angles around Te

Fe-Te1-Fe*	67.33(5)	Fe-Te2-Fe*	70.78(3)
Fe-Te1-Fe#	71.58(4)		

[a] The six Fe atoms form a trigonal antiprism. The labels Fe and Fe* refer to iron atoms in the same basal plane, Fe# refers to an iron atom in the opposite basal plane. [b] Average values; vic = vicinal.

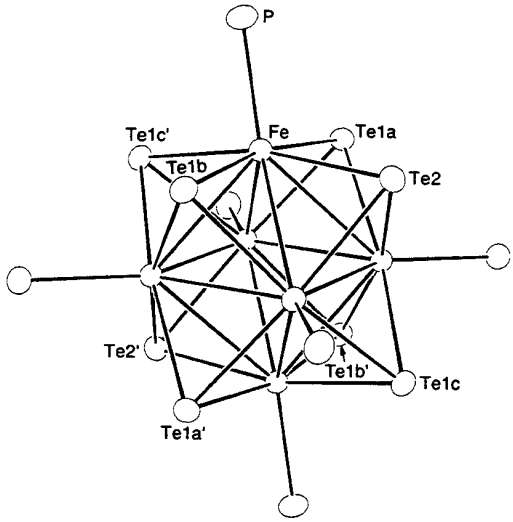

Figure 2. Structure of and labeling for $Fe_6Te_8(PMe_3)_6$, **3**. The structure contains an inversion center. Selected distances and angles are given in Table 3.

Compound **3**, $Fe_6Te_8(PMe_3)_6$, is a member of the M_6E_8 family of "Chevrel-type" clusters.[20-29]

$$6Fe(COT)_2 + 8TePMe_3 \rightarrow Fe_6Te_8(PMe_3)_6 \qquad (2)$$

In this system smaller monodentate phosphines yield larger clusters than do larger phosphines. The next issue is the effect

(13) Nelson, L. L.; Lo, F. Y.-K.; Rae, D.; Dahl, L. F. *J. Organomet. Chem.* **1982**, 309.
(14) Chu, C. T.-W.; Lo, F. Y.-K.; Dahl, L. F. *J. Am. Chem. Soc.* **1982**, *104*, 3409.
(15) Ogino, H.; Tobita, H.; Yanagisawa, K.; Shimoi, M.; Kabuto, C. *J. Am. Chem. Soc.* **1987**, *109*, 5847 and references therein.
(16) Simon, W.; Wilk, A.; Krebs, B.; Henkel, G. *Angew. Chem., Int. Ed. Engl.* **1987**, *26*, 1009.
(17) Barbaro, P.; Bencini, A.; Bertini, I.; Briganti, F.; Midollini, S. *J. Am. Chem. Soc.* **1990**, *112*, 7238.
(18) Brogan, L. E.; Lesch, D. A.; Rauchfuss, T. B. *J. Organomet. Chem.* **1983**, 429.
(19) Roof, L. C.; Kolis, J. W. *Chem. Rev.* **1993**, *93*, 1037.
(20) Saito, T.; Yamamoto, N.; Yamagata, T.; Imoto, H. *J. Am. Chem. Soc.* **1988**, *110*, 1646.
(21) Saito, T.; Yamamoto, N.; Nagase, T.; Tsuboi, T.; Kobayashi, K.; Yamagata, T.; Imoto, H.; Unoura, K. *Inorg. Chem.* **1990**, *29*, 764.
(22) Saito, T.; Yoshikawa, A.; Yamagata, T.; Imoto, H.; Unoura, K. *Inorg. Chem.* **1989**, *28*, 3588.
(23) Cecconi, F.; Ghilardi, C. A.; Midollini, S.; Orlandini, A.; Zanello, P. *J. Chem Soc., Dalton Trans.* **1987**, 831.
(24) Cecconi, F.; Ghilardi, C. A.; Midollini, S.; Orlandini, A. *Polyhedron* **1986**, *5*, 2021.
(25) Diana, E.; Gervasio, G.; Rossetti, R.; Valdemarin, F.; Bor, G.; Stanghellini, P. L. *Inorg. Chem.* **1991**, *30*, 294.
(26) Fenske, D.; Ohmer, J.; Hachengenei, J. *Angew. Chem., Int. Ed. Engl.* **1985**, *24*, 993.
(27) Fenske, D.; Grissinger, A.; Loos, M.; Magull, J. *Z. Anorg. Allg. Chem.* **1991**, *598/599*, 121.
(28) Steigerwald, M. L.; Siegrist, T.; Stuczynski, S. M. *Inorg. Chem.* **1991**, *30*, 2256.
(29) Hessen, B.; Siegrist, T.; Palstra, T.; Tanzler, S. M.; Steigerwald, M. L. *Inorg. Chem.* **1993**, *32*, 5165.

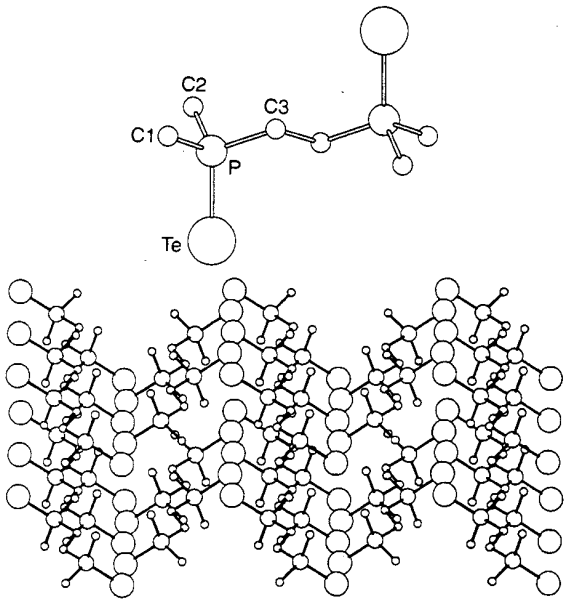

Figure 3. (a) Top: Structure of and labeling for depe·2Te. Selected distances and angles are given in Table 4. (b) Bottom: Crystal packing diagram for depe·2Te.

Table 4. Selected Interatomic Distances (Å) and Angles (deg) in depe·2Te

	Distances		
Te-P	2.357(2)	P-C2	1.796(7)
P-C1	1.825(6)	P-C3	1.803(7)
	Angles		
Te-P-C1	112.9(3)	C1-P-C3	107.04(4)
C1-P-C2	103.24(4)	Te-P-C3	113.63(3)
Te-P-C2	113.93(3)	C2-P-C3	105.3(4)

of multidentate phosphines on the Fe(0)/Te(0) reaction. The most direct experiment in the series would be to allow $Fe(COT)_2$ to react with dmpe·2Te; however, this is hampered by the virtually complete insolubility of dmpe·2Te in toluene. In order to understand this phosphine telluride and its behavior, we prepared it and examined its structure. As distinct from the usual synthesis (direct combination of elemental Te with the phosphine), the most convenient method of preparation of dmpe·2Te is to deliver Te to dmpe in the form of $TePEt_3$ (eq 3). As the dmpe telluride forms, it precipitates from toluene as a microcrystalline solid. (In order to form crystals that are suitable for crystallography, the slow interdiffusion of solutions of the two reagents is required.) The crystallographic description of dmpe·2Te is summarized in Tables 1 and 4 and in Figure 3. The molecular structure is that of a typical phosphine telluride; however, the source of the insolubility of dmpe·2Te is apparent from the crystal packing diagram (Figure 3b): the molecules pack together very tightly in a zipper-like arrangement, aligning the Te atoms from adjacent layers.

$$\text{dmpe} + 2\text{TePEt}_3 \rightarrow \text{dmpe}\cdot 2\text{Te} + 2\text{PEt}_3 \qquad (3)$$

The solubility of dmpe·2Te is greatly enhanced by including a monodentate phosphine such as PEt_3 in the solvent mixture. One can imagine that the dynamic exchange of Te between dmpe and PEt_3 (the transition state for which process contains the $R_3P\cdot Te\cdot PR'_3$ array that is, in the limit of triphenylphosphine, a stable molecule[30,31]) interferes with the formation of the densely packed dmpe·2Te crystal. This feature accounts for the low isolated yield of dmpe·2Te when the latter is prepared from dmpe

(30) Du Mont, W.-W.: Kroth, H.-J. *J. Organomet. Chem.* **1976**, *113*, C35.
(31) Austad, T.; Rød, T.; Åse, K.; Songstad, J.; Norbury, A. H. *Acta Chem. Scand.* **1973**, *27*, 1939.

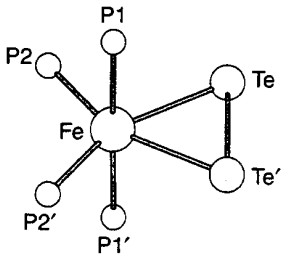

Figure 4. Structure of and labeling for $FeTe_2(depe)_2$, **5**. Selected distances and angles are given in Table 5.

Table 5. Selected Interatomic Distances (Å) and Angles (deg) in $FeTe_2(depe)_2$

	Distances		
Fe-Te	2.660(2)	Fe-P2	2.220(3)
Fe-P1	2.273(3)	Te-Te´	2.674(2)
	Angles		
Te-Fe-Te´	60.35(5)	P1-Fe-P2´	84.3(1)
Te-Fe-P2	94.85(8)	Fe-Te-Te´	59.82(3)
P1-Fe-P2	96.2(2)	Te-Fe-P1´	86.69(9)
Te-Fe-P2	94.85(8)	P1-Fe-P1´	179.2(2)
Te-Fe-P1	92.57(9)	P2-Fe-P2´	110.0(2)
Te-Fe-P2´	155.18(9)		

and $TePEt_3$ and also allows the study of the reactions of $Fe(COT)_2$ with the reaction-equivalent of dmpe·2Te.

When $Fe(COT)_2$ is treated with dmpe and $TePEt_3$ in toluene $(dmpe)_2FeTe_2$, **4**, forms at room temperature (eq 4). The stoichiometry used in this reaction is not critical as **4** forms readily. This compound appears to form good crystals, and we attempted to determine its molecular structure; however, there is disorder in the system and the structure did not refine well. The disorder is with respect to a crystallographic mirror plane that passes approximately through the Fe atom and one of the Te atoms. We hoped that the replacement of dmpe with a closely related bidentate phosphine would give the same inorganic molecular core but one which would pack into regular crystalline order. With this in mind we combined $Fe(COT)_2$ with $TePEt_3$ in the presence of depe. The reaction with depe follows the same path, and $(depe)_2FeTe_2$, **5**, is formed as a crystalline solid (eq 5.) We were able to determine the structure of this material crystallographically, and those results are summarized in Tables 1 and 5 and Figure 4. The iron atom in **5** is coordinated by four phosphorus and two tellurium atoms that form a very distorted octahedron. The Fe-Te and Te-Te distances within the $FeTe_2$ triangle are within the ranges considered normal, although the Fe-Te distance is on the long side and the Te-Te distance is on the short side (see below).

$$Fe(COT)_2 + 2TePEt_3 + 2dmpe \rightarrow (dmpe)_2FeTe_2 \qquad (4)$$

$$Fe(COT)_2 + 2TePEt_3 + 2depe \rightarrow (depe)_2FeTe_2 \qquad (5)$$

The room-temperature absorption spectrum of **5** in the visible region shows three distinct features, all of which are quite intense. There is a strong similarity between this spectrum and that of **4**. On the basis of this, and on the elemental analysis of **4**, and the information to be gleaned from the incomplete X-ray structural refinement, we conclude that **4** is isostructural with **5**.

When the compounds that are formed by dmpe and depe are compared with those based on monodentate phosphines, it is tempting to suggest that cluster growth is very effectively curtailed by the bidentate ligands. This deduction must be modified in view of the formation of $Fe_4Te_6(dmpe)_4$, **6**. Compound **6** is also formed by the reaction of $Fe(COT)_2$, dmpe, and $TePEt_3$; however, in this case a minimum amount of dmpe is used, and the iron reagent and the tellurium reagent are allowed to combine only very slowly (eq 6). The synthesis of **6** is frustratingly unreliable;

$$4Fe(COT)_2 + 6TePEt_3 + 4dmpe \rightarrow Fe_4Te_6(dmpe)_4 \quad (6)$$

however it is repeatable, and we have been able to prepare enough of the material to both determine its structure and measure its magnetization. The crystallographic structure determination is summarized in Tables 1 and 6 and in Figure 5. The structure of **6** is best appreciated as a dimer of $(dmpe)_2Fe_2Te_3$ in which the two subunits are connected by four equivalent Te-to-Fe donor/acceptor bonds. Discounting the potential Fe-Fe interaction (see below), each Fe atom is coordinated by six atoms, the six describing a distorted octahedron. Within each Fe_2Te_3 subunit the three crystallographically distinct Fe-Te bonds are practically identical, and the Fe-Te internuclear distance of 2.586 Å as well within the normal range for covalent bonding.[19,32] The Te-Te internuclear distances are all well over 3 Å; therefore, no Te-Te bonding is evident. Given this, the Fe atoms are conveniently viewed as being in oxidation state III, again ignoring Fe-Fe bonding.

We have measured the magnetization of **1**, **2**, and **6**. Both **1** and **2** are paramagnetic. Above 100 K, each has a temperature-independent effective magnetic moment (8.3 and 8.49 m_B, respectively) that corresponds roughly to 8 parallel spins. Compound **6** is diamagnetic.

We have shown previously[7] that complexes of the form $Fe_4Te_4(PR_3)_4$ undergo pyrolytic condensation to give solid-state tellurides of iron. Here we report that in the same way $Fe_6Te_8(PMe_3)_6$ can be converted to $FeTe_{1\pm x}$ and $(dmpe)_2FeTe_2$ can be converted to $FeTe_2$; thus, all of these Fe/Te molecular and cluster compounds are chemically related to Fe/Te extended compounds.

Discussion

From the results described above it is clear that a variety of clusters result from the interaction of $Fe(COT)_2$ with zerovalent tellurium in the form of $TePR_3$ and that which of that variety one is able to isolate depends critically on which supporting phosphine is used. This suggests a level of reaction control that is available for moderating molecules-to-solids processes and raises the question of why a given phosphine results in a particular cluster. One explanation is crystallization: perhaps all of the cluster types we have observed in this system are present to greater or lesser degrees in all of the reactions, and the particular phosphine that is used selects the particular inorganic cluster core that we observe only because that phosphine-cluster superstructure crystallizes most promptly.

A second explanation is essentially kinetic. When the supporting ligands effectively hide the growing Fe/Te core from the reaction environment, the cluster so-hidden will be kinetically trapped since the ligands must be moved out of the way for further cluster growth to occur. It is reasonable that phosphines that are larger (all else being equal) will cover smaller clusters more effectively than will smaller phosphines. This reasoning predicts that the use of larger phosphines (all else being equal) will result in the isolation of smaller Fe/Te clusters. This rationalization is consistent with what we find.

In the limit of bidentate phosphines one might conjecture that this steric effect would shut down cluster growth entirely and that for this reason the $FeTe_2$ compounds, **4** and **5**, result. The simple explanation based on steric protection is alone not sufficient to rationalize the formation of the $FeTe_2$ compounds, however, since the Te_2 unit in each is still quite exposed to the reaction environment. One might expect that the Te-Te bond would be reactive toward the (essentially) zerovalent iron remaining in the reaction mixture, but in fact neither **4** nor **5** reacts even with added $Fe(COT)_2$. The resolution of this puzzle lies in the electronic structure of the complex. The Te-Te bond in **5** is short for a Te-Te single bond: the bond in **5** is 2.674 Å, while the

Table 6. Selected Interatomic Distances (Å) and Angles (deg) in $Fe_4Te_6(dmpe)_4$

Distances			
Fe-Te1a	2.586(2)	Te1a-Te1′	3.269(2)
Fe-Te1b	2.587(2)	Te1b-Te1′	3.216(2)
Fe-Te1′	2.593(2)	Te1a-Te2	3.655(2)
Fe-Te2	2.585(2)	Te1b-Te2	3.660(2)
Fe-Fe*	2.795(4)		
Fe-P1	2.217(4)	$(Fe\text{-}Te)_{vic}$[a]	2.59
Fe-P2	2.224(4)	$(Te\text{-}Te)_{vic}$[a]	3.45
Angles around Fe			
Te1a-Fe-Te2	89.94(5)	Te1′-Fe-P1	102.2(2)
Te1a-Fe-P1	171.6(2)	P1-Fe-P2	83.6(2)
Te1′-Fe-Te2	160.41(7)	Te1a-Fe-Te1′	76.75(5)
Te1b-Fe-Te2	90.10(6)	Te1b-Fe-Te1′	78.40(5)
Te1a-Fe-Te1b	100.19(6)	Te1′-Fe-P2	102.1(2)
Te1a-Fe-P2	88.5(2)		
Angles around Te			
Fe-Te1a,b-Fe*	65.31(6)	Fe-Te1a-Fe′	99.77(6)
Fe-Te2-Fe*	65.43(6)	Fe*-Te1a-Fe′	98.99(6)

[a] Average values; vic = vicinal.

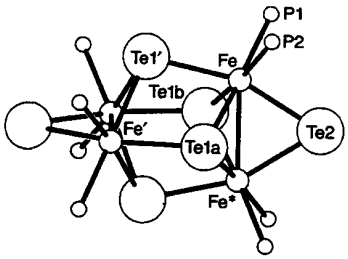

Figure 5. Structure of and labeling for $Fe_4Te_6(dmpe)_4$, **6**. Selected distances and angles are given in Table 6.

Te-Te bond length is 2.715 Å in bis(4-methoxyphenyl) ditelluride,[33] 2.763 Å in $L_5MnTe\text{-}TeMnL_5$,[34] 2.765 Å in $L_4CoTe\text{-}TeCoL_4$,[35] 2.784 Å in $[Cr_4(CO)_{20}(Te_2)]^{2-}$,[36] 2.892 Å in $\{Fe_4Te_4(CO)_{10}\}_2(Te_2)^{2-}$,[36,37] and 2.926 Å in $FeTe_2$ (marcasite structure type).[39] While the bond in **5** is not as short as the bond in free Te_2 (2.59 Å[40]), it is nonetheless short enough to imply a Te-Te bond order greater than one. To the extent that the Te-Te bond order exceeds one, the Fe-Te bonds are not simple covalent bonds. In the limit the Te_2 unit would be a simple donor ligand, and the complex would be better viewed as a trigonal bipyramidal, five-coordinate complex of Fe(0). The description of the Fe in **4** and **5** as zerovalent is supported by the fact that the four phosphorus donors stabilize the low-spin d^8 configuration of zerovalent Fe. This description is also consistent with the lack of reactivity of the Te-Te bond, since such h^2-Te_2 units are apparently not prone to oxidative addition to low-valent metal centers: Di Vaira, Peruzzini, and Stoppioni reported[41] the synthesis and characterization of $(ppp)NiTe_2$ (ppp = bis((2-diphenylphosphino)methyl)phenylphosphine), a complex that is best viewed as a complex of Ni(0) based on the pseudo-tetrahedral coordination around Ni and the short Te-Te bond (2.668 Å). When this complex is treated with $Ni(COD)_2$, the Te-Te moiety

(32) Compton, N. A.; Errington, R. J.; Norman, N. C. *Adv. Organomet. Chem.* **1990**, *31*, 91.
(33) Ludlow, S.; McCarthy, A. E. *J. Organomet. Chem.* **1981**, *219*, 169.
(34) Steigerwald, M. L.; Rice, C. E. *J. Am. Chem. Soc.* **1988**, *110*, 4228.
(35) Steigerwald, M. L.; Siegrist, T; Stuczynski, S. M. *Inorg. Chem.* **1991**, *30*, 4940.
(36) Roof, L. C.; Pennington, W. T.; Kolis, J. W. *Inorg. Chem.* **1992**, *31*, 2056.
(37) Roof, L. C.; Pennington, W. T.; Kolis, J. W. *Angew. Chem., Int. Ed. Engl.* **1992**, *31*, 913.
(38) Huang, S.-P.; Kanatzidis, M. G. *Inorg. Chem.* **1993**, *32*, 821.
(39) Brostigen, G.; Kjekshus, A. *Acta Chem. Scand.* **1970**, *24*, 1925.
(40) Herzberg, G. *Molecular Spectra and Molecular Structure. I. Spectra of Diatomic Molecules*; Van Nostrand Reinhold: New York, 1950; p 576.
(41) Di Vaira, M.; Peruzzini, M.; Stoppioni, P. *Angew. Chem., Int. Ed. Engl.* **1987**, *26*, 916-7.

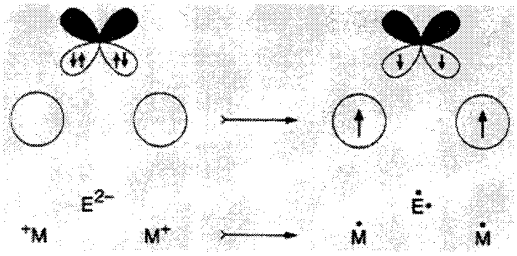

Figure 6. Diagram of the mechanism of anion-mediated superexchange. The central anion ("E") is shown with two perpendicular valence p-orbitals, and each metal atom is represented by a single s-orbital for simplicity. The normal anionic configuration is represented at the left. In this configuration each p-orbital is doubly-occupied. The associated reverse-charge-transfer configuration is shown at the right. In this configuration each E-centered p-orbital is singly-occupied. Since the two p-orbitals are orthogonal, the low energy intra-atomic coupling on E is high-spin. This gives the ferromagnetic coupling of the two metal centers.

simply coordinates in a donor/acceptor sense to the Ni(0) rather than adding to the Ni center oxidatively.

Given these observations, we conclude that the bidentate phosphines quench cluster growth both by covering the metal center sterically and by electronically protecting the zerovalent metal from oxidation.

The magnetic properties of **1**, **2**, and **6** deserve comment. The two Fe_4Te_4 clusters are paramagnetic and have effective moments that are temperature-independent above approximately 100 K[42] and are close to the value of 8.9 m_B that is characteristic of a spin-only paramagnet having $S = 4$ (i.e., 8 parallel spins.) One can rationalize the observed moments in **1** and **2** by noting that in each case each Fe(II) center is in a d^6 configuration in a tetrahedral ligand field and is therefore expected to be (locally) a triplet ($S = 1$). The four triplet Fe centers are then coupled ferromagnetically to give a molecular $S = 4$ ground state.

On the basis of literature precedents, the overall high-spin coupling in a complex such as **1** or **2** is unexpected. For example, the apparently related charge-neutral complexes $Fe_4(NO)_4(m_3\text{-}S)_4$,[14] $Fe_4E_4(CO)_{12}$[13] (E = S, Se), and $Cp_4Fe_4S_4$[11] are all diamagnetic. (The case of $Fe_4(NO)_4(m_3\text{-}S)_4$ is all the more noteworthy since the Fe-Fe distance therein is 2.651 Å-intermediate between the Fe-Fe distances in **1** and **2**. Presuming that direct Fe-Fe two-electron covalent bonding is responsible for the diamagnetic coupling of the Fe(I) centers in $Fe_4(NO)_4(m_3\text{-}S)_4$, one would expect, on the basis of internuclear distances, that the same Fe-Fe bonding, and therefore overall diamagnetism, would occur in **1** and **2**.) In the other $Fe_4Te_4L_4$ complexes for which the information is available ($Fe_4Te_4[EPh]_4^{3-}$, E = S, Te), the antiferromagnetic coupling of the Fe centers is significant.[17]

Superexchange accounts for the ferromagnetic coupling of the Fe centers in **1** and **2**. According to the accepted description of anion-mediated superexchange,[43,44] when the metal-anion-metal internuclear angle is 90° the sense of the metal-metal spin coupling is ferromagnetic. The Fe-Te-Fe angles in **1** and **2** are significantly less than 90°, but the same electronic coupling mechanism is implied and ferromagnetic superexchange is anticipated. This superexchange interaction is represented in Figure 6.

The question arises of why such ferromagnetic coupling in not observed in other Fe_4E_4 clusters. One reason is that the strength of the superexchange interaction is determined in part by the energetic accessibility of the reverse charge transfer that is implied by the configuration shown in Figure 6. This configuration is more accessible the closer the metal and the anion are in electronegativity. Since Fe and Te are closer in electronegativity than Fe and S, the ferromagnetic coupling is expected to be stronger in Fe_4Te_4 clusters than in Fe_4S_4 clusters. If the reverse charge transfer is energetically inaccessible, then antiferromagnetic coupling is expected to dominate *via* conventional through-bond coupling (albeit in this case "through-lone pair" coupling).

Table 7. Comparison of Fe_2Te_3 Fragments in FeTe and $Fe_4Te_6(dmpe)_4$

	FeTe[a]	Fe_4Te_6-(dmpe)$_4$		FeTe[a]	Fe_4Te_6-(dmpe)$_4$
r(Fe-Te) (Å)	2.609	2.586	*q*(Fe-Te-Fe) (deg)	65.3	65.6
q(Te-Fe-Te) (deg)	93.5	93.4	*r*(Fe-Fe) (deg)	2.83	2.80

[a] Values based on data from refs 3 and 45.

Another reason for the ferromagnetic coupling in **1** and **2** is the high local spin state ($S = 1$) on each Fe. The coupling between the Fe-centered Fe-Te bonding electrons and the nonbonding (yet magnetically active) d electrons on the same Fe atom is stronger the larger the number of high-spin coupled d electrons there are. Since this spin-polarization is one of the components of superexchange, the ferromagnetic coupling is expected to weaken as electrons are removed from the Fe centers. This is a plausible explanation for the increased importance of antiferromagnetic coupling in $Fe_4Te_4(EPh)_4^{3-}$.

The diamagnetism of **6** implies the antiferromagnetic coupling of the Fe(III) centers. The antiferromagnetic coupling can be due either to the formation of direct Fe-Fe bonds or to superexchange. The shorter Fe-Fe internuclear distance in **6** (2.795 Å) is long for a direct Fe-Fe covalent bond, but it is within the reported range. (For example, the Fe-Fe bond in $[(h^3\text{-}C_3H_5)\text{-}Fe(CO)_3]_2$ is 3.138 Å.[45]) As mentioned above, the conventional description of superexchange would predict ferromagnetic coupling of the Fe centers in **6** since the Fe-Te-Fe angle is less than 90°, therefore direct Fe-Fe bonding seems the more plausible reason for the observed antiferromagnetic ground state.

Note that even though the Fe-Fe internuclear distances are shorter in **1** and **2** than in **6**, our data indicate that covalent bonds exist between the Fe centers in the latter but not in the former.

We have shown that complexes of the form $Fe_4Te_4(PR_3)_4$, $Fe_6Te_8(PR_3)_6$, and $FeTe_2(PR_3)_4$ can all be converted to corresponding Fe_xTe_y solid-state compounds. We have not been able to isolate **6** in sufficient quantity to test its conversion to FeTe; however, we are confident that that molecules-to-solids process will occur. Since these chemical relationships exist between the clusters and the solids, we sought other comparisons and contrasts between the molecular materials and their extended-solid relatives. The most striking structural relationship between any of the clusters we report here and the corresponding extended solid occurs in the case of **6**. The Fe_2Te_3 subunit that constitutes the core of **6** can be found directly in the NiAs-type FeTe solid.[46] Crystalline $Fe_{1-x}Te$ (NiAs structure type) can be viewed as being constructed by Fe-centered Te_6 octahedra. The Fe_2Te_3 unit is found in the FeTe structure, the Te_3 triangle being a single face of a Te_6 octahedron that is shared between the two Fe centers. The Fe-Fe internuclear direction in the Fe_2Te_3 unit corresponds to the *c*-direction in the NiAs-type solid. The two Fe_2Te_3 fragments (one from $Fe_4Te_6(dmpe)_4$, the other from FeTe[3,4,46]) are compared in Table 7. The numerical comparison shows that the two structures are quite similar.

(42) The low-temperature magnetic behavior of these materials will be reported separately.

(43) Boudreaux, E. A.; Mulay, L. N. *Theory and Applications of Molecular Paramagnetism*, Wiley & Sons: New York, 1976.

(44) Rao, C. N. R.; Gopalakrishnan, J. *New Directions in Solid State Chemistry*; Cambridge University Press: Cambridge, U.K., 1986; Chapter 6.

(45) Putnik,C. F.; Welter, J. J.; Stucky, G. D.; D'Aniello, M.J., Jr.; Sosinski, B. A.; Kirner, J. F.; Muetterties, E. L. *J. Am. Chem. Soc.* **1978**, *100*, 4107.

(46) Useful descriptions of the NiAs structure are included in the following texts. (a) West, A. R. *Solid State Chemistry and Its Applications;* John Wiley & Sons: Chichester, U.K., 1984. (b) Wells, A. F. *Structural Inorganic Chemistry*; Clarendon Press: Oxford, U.K., 1984.

In this case the cluster-to-solid similarity is more than just structural. The ideal NiAs structure is described as an hexagonally close-packed array of anions in which the octahedral interstitial sites are occupied by the cations. Assuming hard sphere atoms, this predicts a crystallographic *c/a* ratio of 1.633.[47] Few metal chalcogenides or pnictides show this ideal value of *c/a*. Most show *c/a* ratios less than 1.633, and the departure from the ideal is rationalized by the presence of metal-metal bonding along the *c*-direction. This metal-metal bonding shrinks the *c*-axis and thereby leads to values of *c/a* less than the ideal. The Fe-Fe vector in the Fe_2Te_3 fragment of FeTe referred to in Table 7 is coincident with the *c*-direction, and therefore, the metal-metal bonding implied by (*c/a*) = 1.487 in FeTe corresponds to the Fe-Fe covalent bonding between these two Fe atoms. Thus, the diamagnetism of **6** (which implies Fe-Fe covalent bonding in **6**) and the lattice contraction in FeTe (which implies Fe-Fe covalent bonding along the *c*-direction in FeTe[48]) are distinctly related.

Conclusion

We have found that the reaction of $Fe(COT)_2$ with $TePR_3$ leads to solid-state iron tellurides, and that when the reaction conditions are moderated, molecular compounds can be retrieved from the mixture. As a general rule, the use of larger phosphines leads to lower nuclearity molecular clusters. Bidentate phosphines also tend to yield small molecular compounds. The Fe(II)-based clusters $Fe_4Te_4(PR_3)_4$ (R = ethyl, isopropyl) are high-spin compounds while the Fe(III)-based compound $Fe_4Te_6(dmpe)_4$ is diamagnetic, showing direct Fe-Fe bonding. The latter compound is clearly identifiable as a fragment of FeTe in the NiAs modification.

(47) Reference 45a, p 250.
(48) Terzieff, P. *Physica B* **1981**, *103*, 158.

Supplementary Material Available: Table S-1, listing crystallographic data for $Fe_4Te_4(P^iPr_3)_4$, $Fe_6Te_8(PMe_3)_6$, dmpe·2Te, $FeTe_2(depe)_2$, and $Fe_4Te_6(dmpe)_4$, Table S-2, listing positional and thermal parameters for $Fe_4Te_4(P^iPr_3)_4$,Table S-3, listing interatomic distances and angles in $Fe_4Te_4(P^iPr_3)_4$, Figure S-1, showing an ORTEP diagram for $Fe_4Te_4(P^iPr_3)_4$, Table S-4, listing positional and thermal parameters for $Fe_6Te_8(PMe_3)_6$, Table S-5, listing interatomic distances and angles in $Fe_6Te_8(PMe_3)_6$, Figure S-2, showing an ORTEP diagram for $Fe_6Te_8(PMe_3)_6$, Table S-6, listing positional and thermal parameters for dmpe·2Te, Table S-7, listing interatomic distances and angles in dmpe·2Te, Figure S-3, showing an ORTEP diagram for dmpe·2Te, Table S-8, listing positional and thermal parameters for $FeTe_2(depe)_2$, Table S-9, listing interatomic distances and angles in $FeTe_2(depe)_2$, Figure S-4, showing an ORTEP diagram for $FeTe_2(depe)_2$, Table S-10, listing positional and thermal parameters for $Fe_4Te_6(dmpe)_4$, Table S-11 listing interatomic distances and angles in $Fe_4Te_6(dmpe)_4$, and Figure S-5, showing an ORTEP diagram for $Fe_4Te_6(dmpe)_4$ (28 pages). Ordering information is given on any current masthead page.